

RESEARCH REPORT

Histological and magnetic resonance analysis of sciatic nerves in the tellurium model of neuropathy

Teresa W. C. Pun¹, Ewa Odrobina², Qing-Gui Xu^{1,4}, Toby Y. J. Lam³, Catherine A. Munro^{1,4}, Rajiv Midha⁵, and Greg J. Stanisz^{2,3}

¹Neuroscience Research and Division of Neurosurgery; ²Imaging Research, Sunnybrook and Women's College Health Sciences Center; ³Department of Medical Biophysics; ⁴Department of Surgery, University of Toronto, Toronto, Ontario; and ⁵Department of Clinical Neurosciences and Neuroscience Research Group, Division of Neurosurgery, University of Calgary, Alberta, Canada

Abstract Ingestion of tellurium (Te), a toxic element, produces paralysis of the hind limbs in weanling rats that is due to temporary, segmental demyelination of the sciatic nerves bilaterally. Weanling rats were fed a 1.1% elemental Te diet and sacrificed at various time points for histological and magnetic resonance (MR) analysis of the sciatic nerves. No controls exhibited impairments of the hind limbs, whereas Te-treated animals became progressively impaired with increased Te exposure. Toluidine blue-stained nerve sections of Te-treated animals showed widened endoneurial spaces, disrupted myelin sheaths, swollen Schwann cells, and a few instances of axonal degeneration. Te decreased healthy myelin by 68% and increased percent extracellular matrix by 45% on day 7. MR experiments showed a decrease in the area of the short T_2 component, an increase in average T_1 , and an increase in the position of the intermediate T_2 component in Te-treated nerves. The correlation coefficient for healthy myelin and average T_1 was 0.88 and that for healthy myelin and the area underneath the short T_2 component was 0.77. The area of the short T_2 component has been postulated as the best measure of the process of demyelination.

Key words: axonal loss, demyelination, MRI, sciatic nerves, tellurium

Introduction

Nerve injuries can occur with trauma, compression syndromes, and systemic illnesses (i.e., diabetes mellitus). A brachial plexus avulsion involves inflammation, demyelination, and axonal loss and requires immediate surgical repair (Glasby and Hems, 1995). In contrast, multiple sclerosis (MS) demonstrates the same three processes, but up to 70% of MS lesions undergo

some degree of remyelination (Stangel, 2004). There is a need for new technologies that can identify and quantify the contribution of inflammation, demyelination, and axonal loss to the injured state. This knowledge will improve our understanding of how nerve pathology is maintained and direct future therapies.

Recent advances in magnetic resonance imaging (MRI) have shown that MR parameters are sensitive to changes in tissue microstructure that reflect disease. Lesions are visualized as a different shade of gray when compared to normal tissue; these changes reflect differences in signal strength in the tissues. Conventional MR parameters, including T_1 and T_2 relaxation times, are dependent on the tissue under investigation and describe the time required for protons in water to return

Address correspondence to: Greg J. Stanisz, PhD, Imaging Research, Sunnybrook and Women's College Health Sciences Center, Rm S656, 2075 Bayview Avenue, Toronto, ON, Canada M4N 3M5. Tel: +1-416-480-5725; Fax: +1-416-480-5714; E-mail: stanisz@sten.sunnybrook.utoronto.ca

to a equilibrium state following stimulation by a radio-frequency (RF) pulse. Most tissues consist of $70 \pm 10\%$ water, and most observable MR signals are due to the two hydrogen nuclei per water molecule (Bronskill and Graham, 1992). T_1 is the longitudinal or spin-lattice relaxation time and T_2 is the spin-spin or transverse relaxation time. Time averaging occurs because water protons move between different compartments (semi-solid or liquid pools) within a tissue. Water protons must exist within a compartment for a minimal amount of time to enable the acquisition of data within the measurement time scale and to be representative of that compartment (Fenrich et al., 2001). Relaxation times also feature multiple components and are described as having multiple peaks of varying amplitudes and areas. These peaks can correspond to different structural compartments in a tissue. Finally, relaxation time data can be acquired using a variety of RF pulse sequences and different sequences are chosen for their ability to distinguish between different tissues (Jackson et al., 1997).

Quantitative T_1 and T_2 relaxation times can be used to evaluate myelin water, a measure of myelin content, in demyelinating diseases (Bagnato and Frank, 2003). Other work suggests that the area underneath the short, observed T_2 component reflects total myelin content (Webb et al., 2003). The presence of abnormalities in T_2 -weighted images, alongside a clinical presentation indicative of demyelination, is a strong predictor for the development of MS. In chronic MS lesions, repeated low magnetization transfer ratios and T_1 -hypointensity signals are associated with demyelination and/or axonal loss (Miller et al., 1998).

We have completed work with MR parameters in normal, regenerating, and irreversibly damaged nerves in rats, using the cut-and-crush model of Wallerian degeneration (Stanisz et al., 2001). Nerve damage increased average T_1 and T_2 relaxation times. These changes were diminished in the regenerating nerves 4 weeks after injury, whereas these differences were maintained in the cut nerves. Changes in MR parameters were associated with the evidence of inflammation and demyelination in histopathological analysis (Stanisz et al., 2001).

Our previous work utilized the cut-and-crush model (Stanisz et al., 2001; Webb et al., 2003) to probe gross nerve injury. Our current focus is on nerve manipulations that produce either inflammation or demyelination in an effort to parse the relative contributions of each process to the changes seen on MR. We recently completed a study using intraneural injections of tumor necrosis factor (TNF- α) to produce inflammation (with minimal axon loss and demyelination) in rat sciatic nerves (Stanisz et al., 2004). The multicomponent T_2 spectrum showed a slight

decrease in the area of the short T_2 component accompanied by a large shift (increase) in the position of the intermediate T_2 component. We hypothesize that demyelination alone would produce a more dramatic decrease in the short T_2 component with little or no shift of the latter component.

In this work, we utilized the tellurium (Te) model of primary demyelination to assess the effect of demyelination on MR parameters. Te is an element in the periodic table that is toxic to both humans and animals (Lampert et al., 1970). Te ingestion produces paralysis of the hind limbs in weanling rats followed by full motor recovery, despite continuation of the Te diet (Lampert et al., 1970; Lampert and Garrett, 1971; Miyoshi and Takauchi, 1977; Duckett et al., 1979; Said and Duckett, 1981; Said et al., 1981). Te-induced paralysis is due to segmental demyelination of the sciatic nerves bilaterally and subsequent remyelination precedes full motor recovery. Little evidence of inflammation and axonal degeneration has been reported (Lampert et al., 1970; Duckett et al., 1979; Bouldin et al., 1988).

Te induces demyelination via metabolic alterations in the myelinating Schwann cells (Harry et al., 1989). A metabolite of Te, tellurite, inhibits squalene epoxidase, a key enzyme in the cholesterol biosynthesis pathway (Wagner-Recio et al., 1991), resulting in a decreased cholesterol synthesis and the accumulation of squalene (Harry et al., 1989). Cholesterol is required for myelin synthesis, and gene expression studies show reversible reductions in P_0 and myelin basic protein RNA in Te-induced demyelination (Toews et al., 1990; 1991; 1997). The accumulation of squalene is toxic to peripheral myelin sheaths as well (Smialek et al., 1997). Although Te effects are systemic, Te intoxication results in the preferential collapse of the larger internodes by targeting Schwann cells with large myelin volumes (Said et al., 1981; Bouldin et al., 1988), thus primarily affecting the sciatic nerves. During the subsequent phase of remyelination, the relative stability of the smaller internodes and the low myelin production of the new Schwann cells contribute to full motor recovery (Bouldin et al., 1988).

The purpose of this study was to quantify the extent of Te-induced demyelination by histomorphometric assessment and to compare the data with changes in quantitative MR parameters. The utility of a Te model of nervous system disease was also explored.

Materials and Methods

Animal model

Ninety-six weanling, Lewis rats, postnatal day (PD) 11, were obtained from Charles River Canada. Animals

were housed in a standard animal facility with a 12/12 hours light/dark cycle. Litters (including dam) were housed in flat-bottom beta-chip-lined cages and allowed ad libitum standard rat chow (1/2" pellets, Purina Rat Chow 5001) and water. Rats were acclimated for 6 days prior to the onset of the study. All experiments and animal interventions adhered strictly to Canadian Council on Animal Care guidelines.

Study design

Beginning on PD 14, animals were assessed for facility of movement daily. On removal of the dam (PD 17), 62 experimental animals received a diet containing 1.1% elemental Te (1/2" pellets of Purina Rat Chow 5001 with the addition of Te), obtained from Bio-Serv *ad libitum*. Filter cage tops were employed to limit human Te exposure. Following diet onset, animals were euthanized daily (days 1–7) with an intramuscular injection of 300 mg/kg ketamine hydrochloride (0.1 mL/100 g Rogarestic, Rogra-STB) and 30 mg/kg xylazine (20 mg/mL, Bayer Inc.) into the lumbar paraspinal musculature. Following bilateral gluteal and posterior thigh incisions, the sciatic nerves were exposed. Nerve tissue samples (approximately 2 cm long) were harvested from high in the sciatic notch to the branch point. The middle portion (approximately 1.5 cm in length) was reserved for MR analysis; the proximal and distal nerve sections were taken for histopathological analysis. Thirty-four control animals remained on the standard rat chow (1/2" pellets of Purina Rat Chow 5001) and were sacrificed at similar time points in an identical fashion.

Histology

Proximal and distal nerve sections were fixed by immersion in Universal fixative (40% formalin, 25% glutaraldehyde), postfixed with osmium tetroxide, and embedded in Epon-Araldite. Toluidine blue was used to stain 1- μ m-thick cross-sections for light microscopy (Stanisz et al., 2004).

Nerve cross-sections were evaluated using an Olympus BX51 light microscope (Olympus America Inc.) linked to an image analysis system (Image Pro Plus version 4.5, Media Cybernetics). Histomorphometric studies to determine healthy myelin content (defined as thick, undisrupted sheaths) were performed on seven randomly selected, representative fields with an area of 3090 μ m² at \times 1000 magnification. At least 25% of the total cross-sectional area per nerve sample was evaluated. Images were captured using a Cool Snap-Pro camera (Media Cybernetics Inc.), and axons larger than 1 μ m in diameter were analyzed. Healthy myelin content was assessed per field, and the myelin and extracellular matrix volume fractions were calculated as percentages of the total

sampled area, as previously developed in our laboratory (Webb et al., 2003). All data were analyzed using the STATISTICA (1998) software. ANOVAs and Tukey HSD post hoc tests were performed at an α level of 0.05.

MR experiments

Extracted nerve samples were placed in non-protonated fomblin solution (3M, Fluorinert) to avoid dehydration and reduce susceptibility effects. The MR measurements were performed at 20°C and 1.5 T on a 20-cm bore superconducting magnet (Nalorac, Cryogenics Corp.) controlled by an SMIS spectroscopy console (SMIS). Rectangular RF pulses were amplified by an RF amplifier (Model 3205; American Microwave Technology). T_2 relaxation time data were acquired using a Carr-Purcell-Meiboom-Gill sequence with TE/TR = 1/10,000 ms, 2000 even echoes sampled and 100 averages. T_1 relaxation time data were acquired using an inversion recovery sequence with 35 T_1 values logarithmically spaced from 1 to 32,000 ms, with 10 s between each acquisition and the next inversion pulse and two averages.

Results

General observations

No animals in the control group ($N=34$) exhibited abnormalities of the hind limbs during the time course of the study. In contrast, impairments appeared in the Te group ($N=62$) as early as day 1 (24 h on the Te diet) and became more pronounced with time (Fig. 1). By day 4, all Te animals showed mild or considerable impairment of the hind limbs. Mild impairment was characterized as an awkward hopping movement of

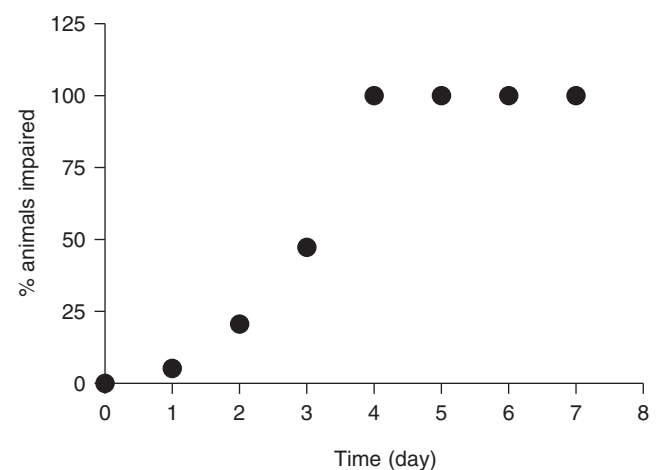


Figure 1. Tellurium (Te)-induced hind limb impairments over time. No control or Te animals, prior to receiving Te, showed motor abnormalities of the hind limbs.

the hind limbs. Considerable impairment was defined as a severe dragging or partial paralysis of the hind limbs. These animals dragged the ventral surface of their hind limbs on the floor and only lifted these limbs in a stepping motion occasionally. Locomotion was largely unaffected because the impaired animals used their forelimbs in a normal fashion. All affected Te animals showed poor toe spacing in the hind feet. Control animals showed normal (wide) toe spacing at all times.

There were no differences in body size or weight before the study (data not shown). However, Te rats were smaller and weighed less than controls, although this was not quantified.

On extraction of the sciatic nerves, there were no visible gross differences between nerves of controls and those of Te animals. All control and 100% of Te animals in days 1–4 survived to study endpoint. Mortality was 22% (two of nine animals), 25% (two of eight animals), and 67% (six of nine animals) in day 5, 6, and 7 Te animals, respectively, presumably because of the Te diet.

Histology

Figure 2 shows representative Toluidine blue-stained cross-sections from control and Te sciatic nerves at days 1–7. Te-treated nerves showed widened endoneurial spaces with more prominent Remak bundles, large Schwann cells, and dramatic alterations in myelin structure, including myelin debris. Some of the Schwann cells appeared swollen with lipid globules, indicative of phagocytosed material. All of these changes were absent in control nerves, which showed thick myelin sheaths and fewer Schwann cells. The axons of Te-treated nerves appeared normal in the earlier stages, but signs of axonal degeneration were present at days 6 and 7 (Fig. 2H).

ANOVA revealed significant differences between control and Te animals on percent myelin and percent extracellular matrix in the sciatic nerve. Te animals showed a significant decrease in healthy myelin content [$F(1,56) = 154.66$, $p < 0.001$] over time (Fig. 3A). Compared to controls, myelin decreased by 20, 22, 34, 47, 42, 62, and 68% on days 1–7, respectively. There was also a main effect of day [$F(6,56) = 4.82$, $p < 0.001$] and a significant group by day interaction [$F(6,56) = 3.58$, $p < 0.005$]. A post hoc Tukey HSD showed differences between days 1 and 6, 1 and 7, 2 and 6, and 2 and 7 ($p < 0.01$) in Te animals.

Te-treated nerves showed a significant increase in total extracellular matrix content [$F(1,56) = 260.15$, $p < 0.001$] over time (Fig. 4A). Compared to controls, extracellular matrix increased by 6, 8, 15, 26, 27, 39, and 45% on days 1–7, respectively. A main effect of day [$F(6,56) = 14.68$, $p < 0.001$] and a significant group

by day interaction [$F(6,56) = 14.74$, $p < 0.001$] were present as well. A post hoc Tukey HSD showed differences between days 1 and 5, 1 and 6, 1 and 7, 2 and 6, 2 and 7, 3 and 6, 3 and 7, 4 and 6, 4 and 7, 5 and 6, and 5 and 7 ($p < 0.05$).

MR experiments

ANOVA showed significant differences between control and Te animals in the area underneath the short T_2 peak, the average T_1 and the position of the intermediate T_2 peak. Figure 5 shows a typical multi-component T_2 spectrum. The area underneath the short observed T_2 component was decreased significantly [$F(1,72) = 14.44$, $p < 0.001$] in Te animals in comparison with controls (Fig. 3B). There was also a main effect of day [$F(6,72) = 5.80$, $p < 0.0001$]. A post hoc Tukey HSD showed significant differences between days 1 and 2, 2 and 3, 2 and 4, 2 and 5, 2 and 6, 2 and 7, 1 and 3, 3 and 4, 3 and 5, 3 and 6, and 3 and 7 ($p < 0.05$) in all animals.

The average T_1 was increased significantly (Fig. 3C) in Te animals, when compared with controls [$F(1,72) = 128.49$, $p < 0.001$]; there was also a significant group by day interaction [$F(6,72) = 0.40$, $p < 0.05$]. A post hoc Tukey HSD demonstrated significant differences between days 1 and 4, 1 and 5, 1 and 6, 2 and 4, 2 and 5, 2 and 6, 2 and 7, and 3 and 6 ($p < 0.05$) in Te animals.

The position of the intermediate T_2 component was increased significantly (Fig. 4B) in Te animals [$F(1,72) = 100.36$, $p < 0.0001$]. There was also a main effect of day [$F(6,72) = 2.96$, $p < 0.05$] and a significant group by day interaction [$F(6,72) = 3.36$, $p < 0.01$].

Correlation

Correlation analysis was performed using histology (percent myelin and extracellular matrix) and MR (average T_1 , position of the intermediate T_2 component, and the area under the short T_2 component) measurements between Te and control animals (all days). Myelin content and the area underneath the short T_2 component had a correlation coefficient of 0.77; myelin and average T_1 were correlated at 0.88; myelin and the position of the intermediate T_2 component were correlated at 0.73, and myelin and extracellular matrix content had a correlation coefficient of 0.98. Extracellular matrix content was correlated with average T_1 at 0.92; extracellular matrix and the position of the intermediate T_2 component had a correlation coefficient of 0.72.

Discussion

The neuropathological changes associated with Te ingestion in weanling rats have been documented

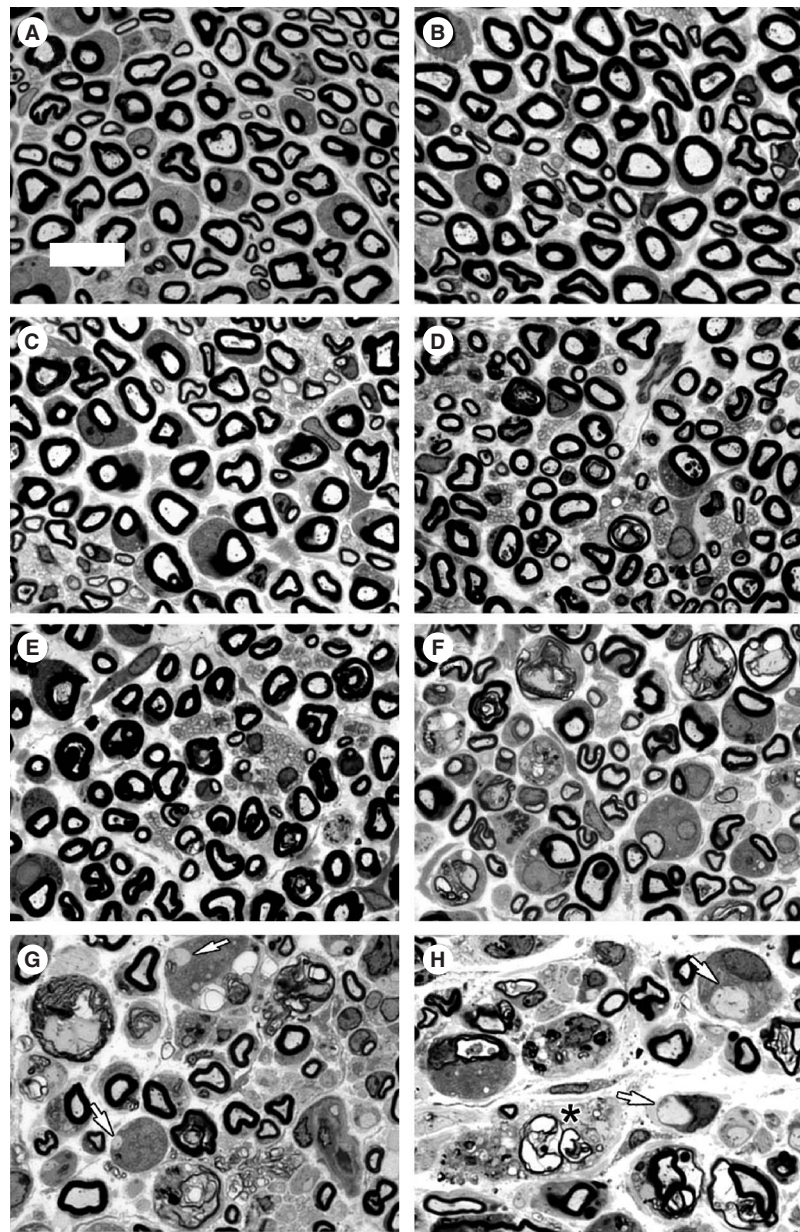


Figure 2. Toluidine blue-stained nerve sections of control (A) and tellurium (Te) animals (B–H) from days 1–7. A is a day 4 control; B is a day 1 Te; C to H are days 2–7, respectively. Control nerves showed no change over time. Te-treated nerves showed increasing abnormalities in the myelin sheath and increased extracellular space beginning on days 3 and 4. Day 4 also featured prominent Remak bundles. Arrows in G and H indicate demyelinated axons, surrounded by large phagocytosing Schwann cells. The asterisk (*) in H shows a degenerating axon. The white spaces are areas of phagocytosed debris, and there is no axon present in this profile. The white bar in A marks 10 μ m.

extensively by previous researchers (Lampert et al., 1970; Lampert and Garrett, 1971; Duckett et al., 1979). In the present study, weanling rats developed partial paralysis of the hind limbs over a 7-day period at a dose of 1.1% elemental Te. No controls or Te animals, prior to receiving the Te diet, exhibited motor abnormalities of the hind limbs. Affected Te animals hopped awkwardly on their hind feet or dragged their hind limbs with narrow, improper toe spacing.

Previous work with Te has been conducted with Long Evans (Lampert et al., 1970; Lampert and Garrett, 1971; Bouldin et al., 1988), Wistar (Duckett et al., 1979; Said and Duckett, 1981; Said et al., 1981), and Sprague–Dawley (Wiley-Livingston and Ellisman, 1982) rats. Our laboratory chose to use Lewis rats because of our prior experience with this strain in similar MR experiments. To minimize mortality, we used a 1.1% elemental Te diet (Lampert and Garrett,

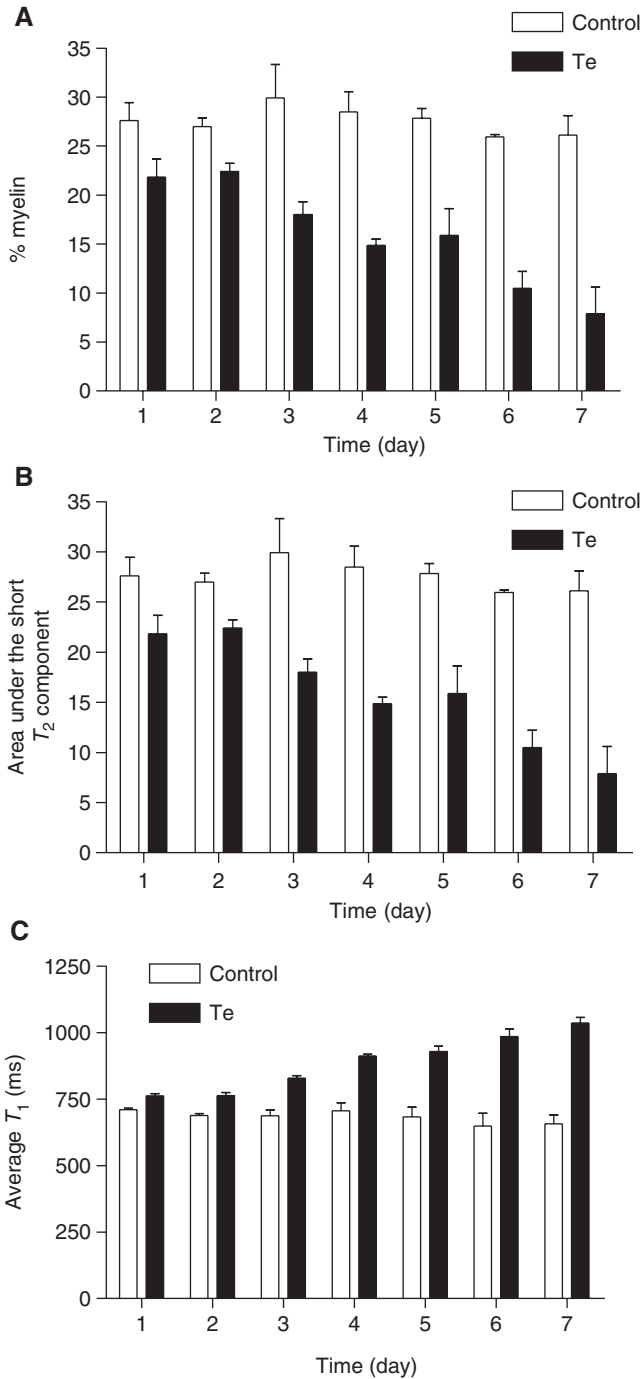


Figure 3. (A) Effect of tellurium (Te) on myelin content. Control and Te-treated nerves were significantly different at $p < 0.001$. Te-treated nerves showed a 11.3% decrease in myelin. Although control nerves showed no change over time, Te-treated nerves showed decreased myelin with increased Te exposure ($p < 0.01$). (B) Effect of Te on the area under the short, observed T_2 component. The T_2 area was significantly decreased in Te animals ($p < 0.001$). (C) Effect of Te on average T_1 . T_1 was significantly increased in Te animals when compared with controls ($p < 0.001$). There was a significant day by group interaction ($p < 0.05$), and a post hoc Tukey HSD showed significant differences between days 1 and 4, 1 and 5, 1 and 6, 2 and 4, 2 and 5, 2 and 6, 2 and 7, and 3 and 6 ($p < 0.05$) in Te animals.

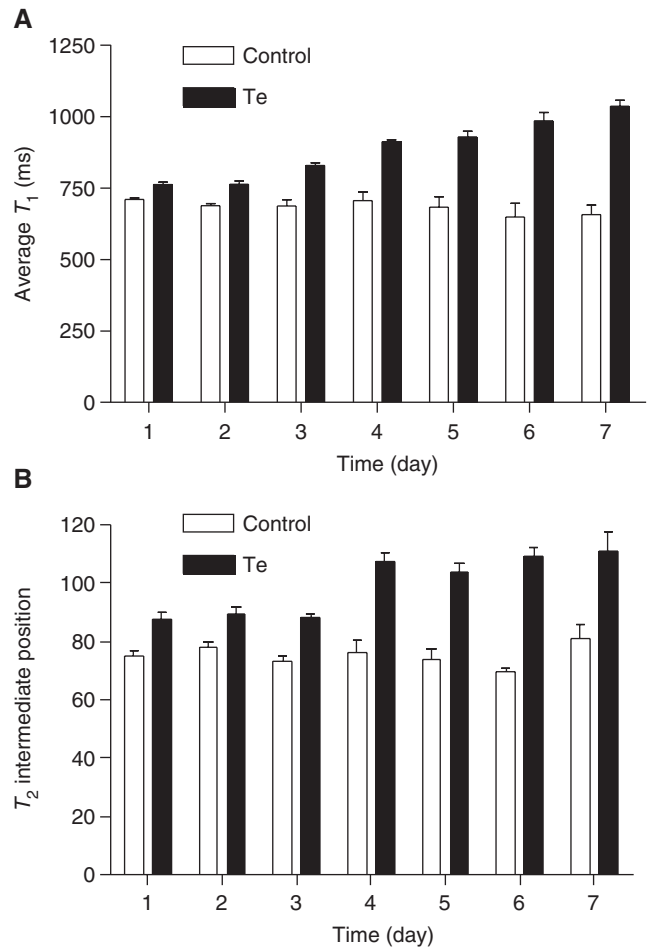


Figure 4. (A) Effect of tellurium (Te) on extracellular matrix content. Te-treated nerves showed a significant 13.8% increase in extracellular matrix ($p < 0.001$). Te-treated nerves showed increased extracellular matrix with increased Te exposure ($p < 0.05$). (B) Effect of Te on the position of the intermediate T_2 component. This magnetic resonance parameter was increased significantly in Te animals ($p < 0.0001$). With increasing Te exposure, the position of the intermediate T_2 component increased correspondingly ($p < 0.01$).

1971), a dose that nevertheless produced a profound paralytic effect (Toews et al., 1990). Although mortality increased after day 5 in our animals, rats of different strains consistently survived to day 10 and beyond on a 1.1% (Lampert et al., 1970) or 1.25% Te diet (Duckett et al., 1979). The results of the present study suggest that Te does not affect all rat strains equally and that Lewis rats may be more susceptible to Te toxicity. This may be due to alterations in the cholesterol biosynthesis pathway or in the mechanisms involved in drug clearance that are specific to Lewis rats. Overall, rats in the Te group were smaller and weighed less than their control counterparts, but observable differences in weight were not noticeable between those Te animals that survived and those that did not. The

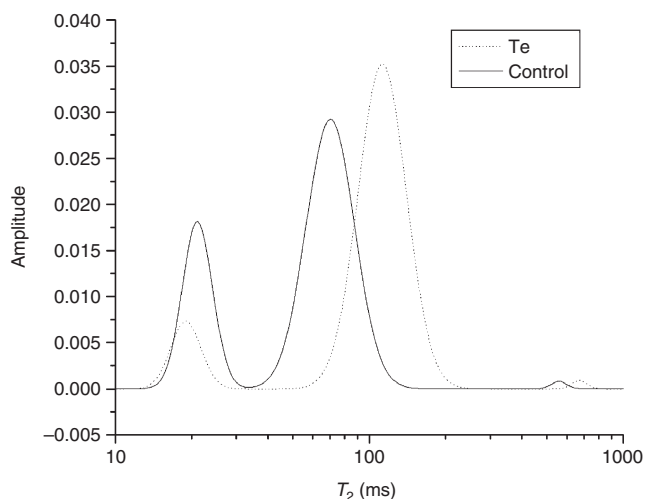


Figure 5. Multicomponent T_2 spectrum. The peaks are designated as a, b, and c. Healthy myelin is associated with the area underneath the first, short peak, T_{2a} . Inflammation is associated with the position (right shift) of the second peak, T_{2b} . Tellurium treatment decreased the area underneath short (20 ms) and increased the position of intermediate (60–105 ms).

difference in weight between groups may be more attributable to the fact that control animals gained weight steadily, whereas Te animals did not. Possible explanations for Te-associated mortality include disrupted nerve signaling to critical organs and effects on the central nervous system (CNS). Although the sciatic nerve was preferentially affected, nerves involved with signaling to organs critical for life (heart and diaphragm) and spinal cord and brain tissue should be harvested and investigated for histopathological changes as well.

Researchers studying Te toxicity have also used subcutaneous injections of squalene to directly assess the effects of this accumulated metabolite on neural structure. They found changes in both the peripheral nervous system (PNS) and CNS. PNS changes included damage to Schwann cells, demyelination, and lipid-like deposits between myelin lamellae. The latter may compress axons and lead to functional deficits. CNS changes included mild swelling of mitochondria and astrocytes, accumulation of the same lipid-like droplets in some neurons in the cerebral cortex and hippocampus, and some myelin sheath disruption in cerebral white matter (Smialek et al., 1997; Gajkowska et al., 1999). Further investigation is required to explore the selective vulnerability of Lewis rats to premature death from Te toxicity and to elucidate the cause of death, be it systemic, peripheral nerve, or CNS related.

Histological analysis of the control nerves was unremarkable throughout the duration of the study. In contrast, Te-treated nerves showed increased extracellular space, swollen Schwann cells, and demyelinated axons. The former was also exemplified by the

presence of Remak bundles, bundles of unmyelinated peripheral axons, likely because of the widened extracellular space. Schwann cells increase dramatically in number following Te treatment to (1) phagocytose damaged myelin (along with endoneurial macrophages) and (2) participate in the remyelination process (Berciano et al., 1998). The increase in Schwann cell numbers is regulated, in part, by apoptosis (Berciano et al., 1998), but the Schwann cells in this study did not demonstrate the typical shrunken profile of a cell undergoing programmed cell death. The larger appearance of these cells was likely a result of Te-induced damage and/or ongoing phagocytic activity. Although large, phagocytosing Schwann cells and macrophages may appear similar at the light microscope level, the existing literature (including electron microscopy studies) provides support that these cells are most likely Schwann cells (Duckett et al., 1979; Said et al., 1981). Macrophage proliferation and infiltration would be more suggestive of an inflammatory process, and Te is associated with little or no inflammation (Lampert et al., 1970; Duckett et al., 1979; Bouldin et al., 1988).

Te has been described as a model of primary demyelination with little axonal degeneration (Lampert et al., 1970; Lampert and Garrett, 1971; Said et al., 1981). The histology results in this study showed evidence of axonal loss in Wallerian degeneration profiles, although this was not quantified. Axonal degeneration may also be inferred from an increase in extracellular matrix. This difference is even more pronounced when the increase in Schwann cell numbers (though not quantified) is taken into consideration. Although the extent of axon loss warrants further investigation, Te remains a model of demyelination first and axonal degeneration second. Histological analysis showed more evidence of demyelination than Wallerian degeneration, and this confirms the work done by earlier researchers (Lampert et al., 1970; Lampert and Garrett, 1971; Said et al., 1981).

In this study, we quantified myelin loss in the Te model of demyelination and showed that reductions of healthy myelin by 22–68% were associated with behavioural dysfunction. It is unclear whether axonal degeneration contributes significantly to behavioural impairment. However, previous researchers have demonstrated full remyelination and recovery of function in 10–14 days (Lampert et al., 1970; Lampert and Garrett, 1971; Duckett et al., 1979; Said et al., 1981). Axonal regeneration would likely warrant a longer recovery period, as evidenced by the poor outcomes associated with nerve damage in clinical cases (Midha and Kline, 1998). Our study was limited to 7 days of Te exposure, and there was little evidence of remyelination at this stage. Extending the study in a different rat

strain may be helpful to document the hypothesized reversal of changes in the MR parameters.

Less than 10% of animals were impaired on day 1, yet myelin was reduced by 19% at this time. Changes in tissue microstructure are evident prior to the clinical manifestation of disease, and the non-invasive detection of these changes will aid in a rapid diagnosis in patient populations.

The *ex vivo* MR experiments showed changes in three MR parameters in Te-treated nerves. The area underneath the short T_2 component was reduced; average T_1 and the position of the intermediate T_2 component were increased. In this experiment, we assessed only healthy myelin; reductions in myelin, as determined by histological analysis, were correlated with reductions in the area under the short, observed T_2 component. Although our previous experiments (Webb et al., 2003) did not distinguish between healthy and diseased myelin, the current study suggests that changes in the short T_2 peak reflect changes in the amount of healthy myelin. This is important clinically because healthy myelin can indicate functional recovery (Scolding and Franklin, 1997). In contrast, a measure that combines both healthy and disrupted myelin would be of little diagnostic value.

Average T_1 and the position of the intermediate T_2 component showed increases in both inflammation (Stanisz et al., 2004) and demyelination (current study). Although the two disease processes cannot be distinguished by average T_2 alone, the position of the intermediate T_2 component is more increased with inflammation (Stanisz et al., 2004).

The results of the TNF- α study (Stanisz et al., 2004) and the Te experiments (current study) demonstrate that differences exist between demyelination and inflammation on MR parameters. The area underneath the short T_2 component reflects myelin content, and the position of the intermediate component is associated with inflammation. The contribution of axonal degeneration to the changes seen in this study needs to be assessed to further differentiate these three processes. Previous work using the cut-and-crush model of Wallerian degeneration has shown that increases in the position of the intermediate T_2 component reflect axonal loss (Stanisz et al., 2001). Thus, conventional MR parameters can differentiate between demyelination and inflammation, but not inflammation and axonal loss. As our understanding of these MR signals increases, so will our ability to interpret neural tissue pathology with an MR spectrum.

References

- Bagnato F, Frank JA (2003). The role of nonconventional magnetic resonance imaging techniques in demyelinating disorders. *Curr Neurol Neurosci Rep* 3:238–245.
- Berciano MT, Calle E, Fernandez R, Lafarga M (1998). Regulation of Schwann cell numbers in tellurium-induced neuropathy: apoptosis, supernumerary cells and internodal shortening. *Acta Neuropathol (Berl)* 95:269–279.
- Bouldin TW, Samsa G, Earnhardt TS, Krigman MR (1988). Schwann cell vulnerability to demyelination is associated with internodal length in tellurium neuropathy. *J Neuropathol Exp Neurol* 47:41–47.
- Bronskill MJ, Graham SJ (1992). NMR characteristics of tissue. In: *The Physics of MRI*. 1992 AAPM Summer School Proceedings. Bronskill MJ, Sprawls P (Eds). American Institute of Physics, New York, pp 32–55.
- Duckett S, Said G, Streletz LG, White RG, Galle P (1979). Tellurium-induced neuropathy: correlative physiological, morphological and electron microprobe studies. *Neuropathol Appl Neurobiol* 5:265–278.
- Fenrich FR, Beaulieu C, Allen PS (2001). Relaxation times and microstructures. *NMR Biomed* 14:133–139.
- Gajkowska B, Smialek M, Ostrowski RP, Piotrowski P, Frontczak-Baniewicz M (1999). The experimental squalene encephaloneuropathy in the rat. *Exp Toxicol Pathol* 51:75–80.
- Glasby MA, Hems TE (1995). Repairing spinal roots after brachial plexus injuries. *Paraplegia* 33:359–361.
- Harry GJ, Goodrum JF, Bouldin TW, Wagner-Recio M, Toews AD, Morell P (1989). Tellurium-induced neuropathy: metabolic alterations associated with demyelination and remyelination in rat sciatic nerve. *J Neurochem* 52:938–945.
- Jackson EF, Ginsberg LE, Schomer DF, Leeds NE (1997). A review of MRI pulse sequences and techniques in neuroimaging. *Surg Neurol* 47:185–199.
- Lampert PW, Garrett RS (1971). Mechanism of demyelination in tellurium neuropathy. Electron microscopic observations. *Lab Invest* 25:380–388.
- Lampert P, Garro F, Pentschew A (1970). Tellurium neuropathy. *Acta Neuropathol (Berl)* 15:308–317.
- Midha R, Kline DG (1998). Evaluation of the neuroma in continuity. In: *Management of Peripheral Nerve Problems*. Omer GE Jr, Spinner M, Van Beek AL (Eds). W.B. Saunders Company, Philadelphia, pp 319–327.
- Miller DH, Grossman RI, Reingold SC, McFarland HF (1998). The role of magnetic resonance techniques in understanding and managing multiple sclerosis. *Brain* 121:3–24.
- Miyoshi K, Takauchi S (1977). Chronic tellurium intoxication in rats. *Folia Psychiatr Neurol Jpn* 31:111–118.
- Said G, Duckett S (1981). Tellurium-induced myelinopathy in adult rats. *Muscle Nerve* 4:319–325.
- Said G, Duckett S, Sauron B (1981). Proliferation of Schwann cells in tellurium-induced demyelination in young rats. A radioautographic and teased nerve fiber study. *Acta Neuropathol (Berl)* 53:173–179.
- Scolding NJ, Franklin RJM (1997). *Baillieres Clin Neurol* 6:525–548.
- Smialek M, Gajkowska B, Ostrowski RP, Piotrowski P (1997). Experimental squalene encephaloneuropathy in the rat. *Folia Neuropathol* 35:262–264.
- Stangel M (2004). Remyelinating and neuroprotective treatments in multiple sclerosis. *Expert Opin Investig Drugs* 13:331–347.
- Stanisz GJ, Midha R, Munro CA, Henkelman RM (2001). MR properties of rat sciatic nerve following trauma. *Magn Reson Med* 45:415–420.
- Stanisz GJ, Webb S, Munro CA, Pun T, Midha R (2004). MR properties of excised neural tissue following experimentally induced inflammation. *Magn Reson Med* 51: 473–479.

- Toews AD, Eckermann CE, Roberson MD, Lee SY, Morell P (1991). Primary demyelination induced by exposure to tellurium alters mRNA levels for nerve growth factor receptor, SCIP, 2',3'-cyclic nucleotide 3'-phosphodiesterase, and myelin proteolipid protein in rat sciatic nerve. *Brain Res Mol Brain Res* 11:321–325.
- Toews AD, Lee SY, Popko B, Morell P (1990). Tellurium-induced neuropathy: a model for reversible reductions in myelin protein gene expression. *J Neurosci Res* 26:501–507.
- Toews AD, Roe EB, Goodrum JF, Bouldin TW, Weaver J, Goines ND, Morell P (1997). Tellurium causes dose-dependent coordinate down-regulation of myelin gene expression. *Brain Res Mol Brain Res* 49:113–119.
- Wagner-Recio M, Toews AD, Morell P (1991). Tellurium blocks cholesterol synthesis by inhibiting squalene metabolism: preferential vulnerability to this metabolic block leads to peripheral nervous system demyelination. *J Neurochem* 57:1891–1901.
- Webb S, Munro CA, Midha R, Stanisz GJ (2003). Is multicomponent T2 a good measure of myelin content in peripheral nerve? *Magn Reson Med* 49:638–645.
- Wiley-Livingston CA, Ellisman MH (1982). Return of axonal and glial membrane specializations during remyelination after tellurium-induced demyelination. *J Neurocytol* 11:65–80.

Copyright of Journal of the Peripheral Nervous System is the property of Blackwell Publishing Limited and its content may not be copied or emailed to multiple sites or posted to a listserv without the copyright holder's express written permission. However, users may print, download, or email articles for individual use.